Electronic Supplementary Information

Triggering Phase Transition and Capacity Enhancement of Nb_2O_5 for Fast-Charging Lithium-ion Storage

Fei Shen,[1,2,5] Zhongti Sun,[1,2,5] Liang Zhao,[1,5] Yuanhua Xia,[3,5] Yanyan Shao,[1,2,] Jingsheng Cai,[1,2] Shuo Li,[1,2] Chen Lu,[1,2] Xiaoling Tong,[1,2] Yu Zhao,[1,2] Jingyu Sun,[1,2,4] Yuanlong Shao[1,2,4]*

[1]College of Energy, Soochow Institute for Energy and Materials InnovationS (SIEMIS), Jiangsu Provincial Key Laboratory for Advanced Carbon Materials and Wearable Energy Technologies, Soochow University, 215006 Suzhou, P. R. China

[2]SUDA-BGI Collaborative Innovation Center, Soochow University, Suzhou 215006, P. R. China.

[3]Key Laboratory of Neutron Physics, Institute of Nuclear Physics and Chemistry, China Academy of Engineering Physics, Mianyang 621999, People's Republic of China

[4]Beijing Graphene Institute (BGI), 100095 Beijing, P. R. China

[5]These authors contributed equally.

***CORRESPONDING AUTHOR NOTE:**

Prof. Yuanlong Shao, E-mail: ylshao@suda.edu.cn

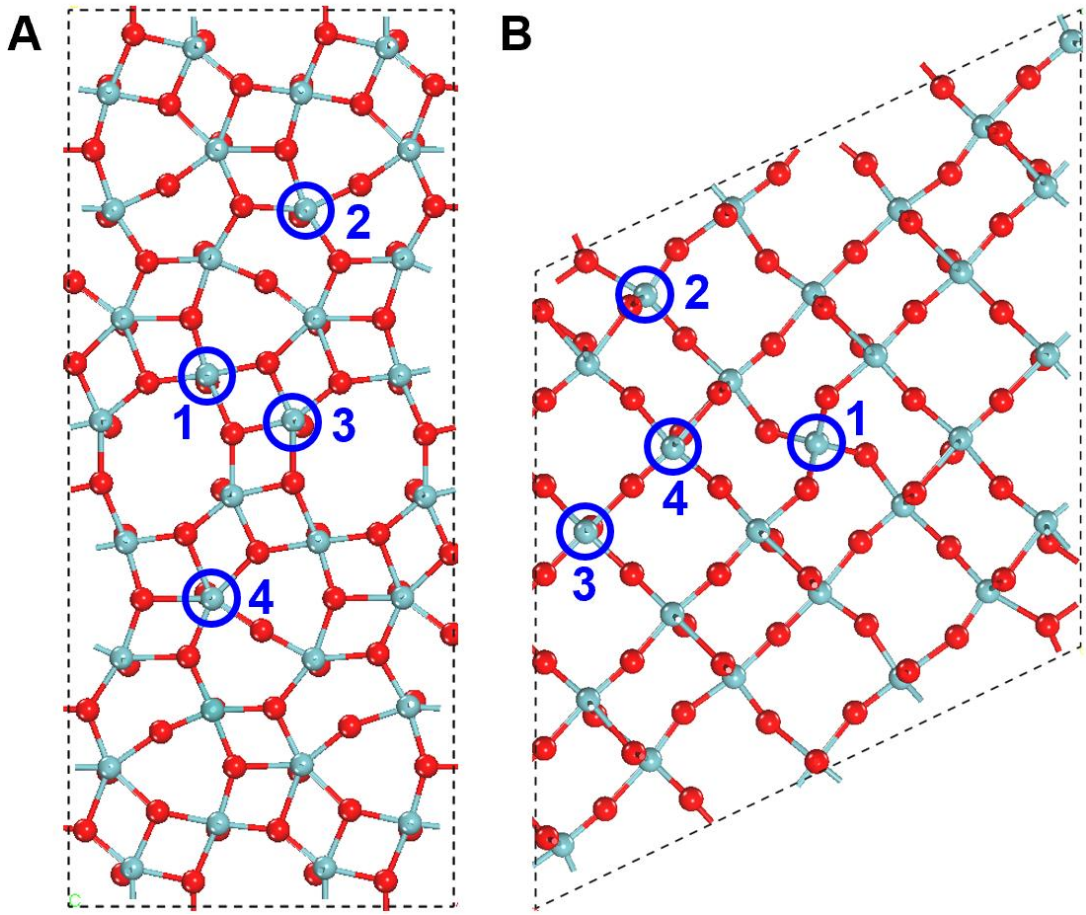

Fig. S1. The possible substituting sites for Mo, marked as “1, 2, 3, 4” for the T phase with periodically repeating (2×1×1) supercell A and H phase unit cell B, respectively. For the T-Nb_2O_5 phase, “1” configuration is lower than “2”, “3”, “4” site models by 0.06, 0.13 and 0.33 eV, respectively. For the H-Nb_2O_5 phase, “1” site owns the lowest energy among others by 0.7 eV for “2” and “3” site, by 0.74 eV for “4” locations.

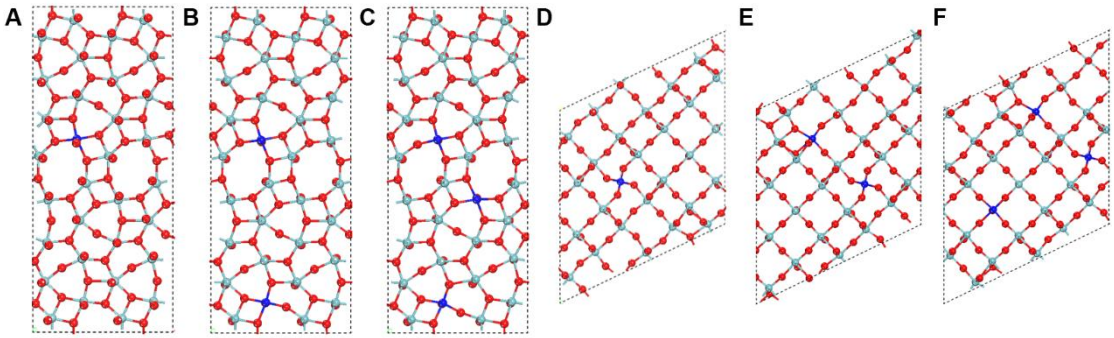

Fig. S2. The possible configurations with ratios of Mo/Nb of 0.032 A 0.067 B and 0.010 C in the T phase; with ratios of Mo/Nb of 0.040 D, 0.077 E and 0.120 F in the H phase. Light blue, blue, and red balls indicate Nb, Mo, and O atoms, respectively.

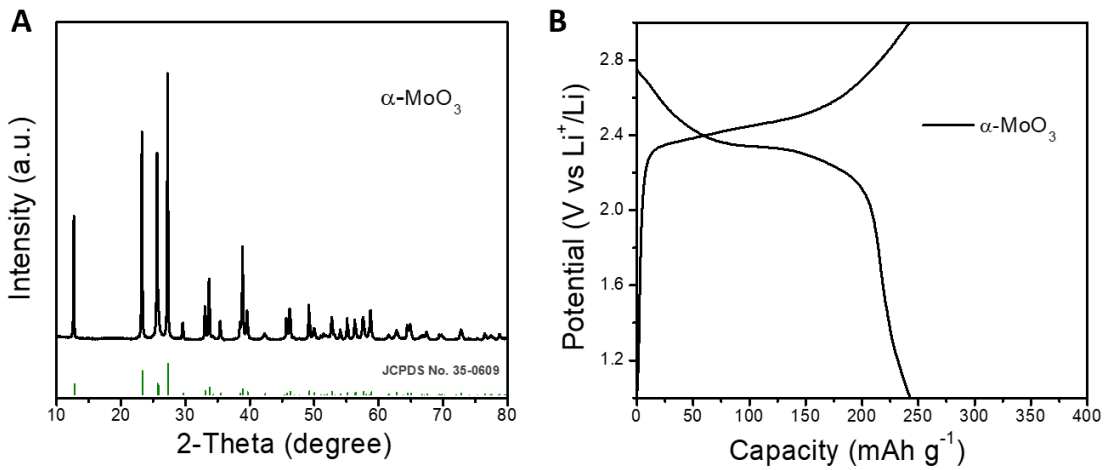

Fig. S3. A, XRD pattern of α-MoO_3, and B, charge/discharge curves of α-MoO_3//Li half cell.

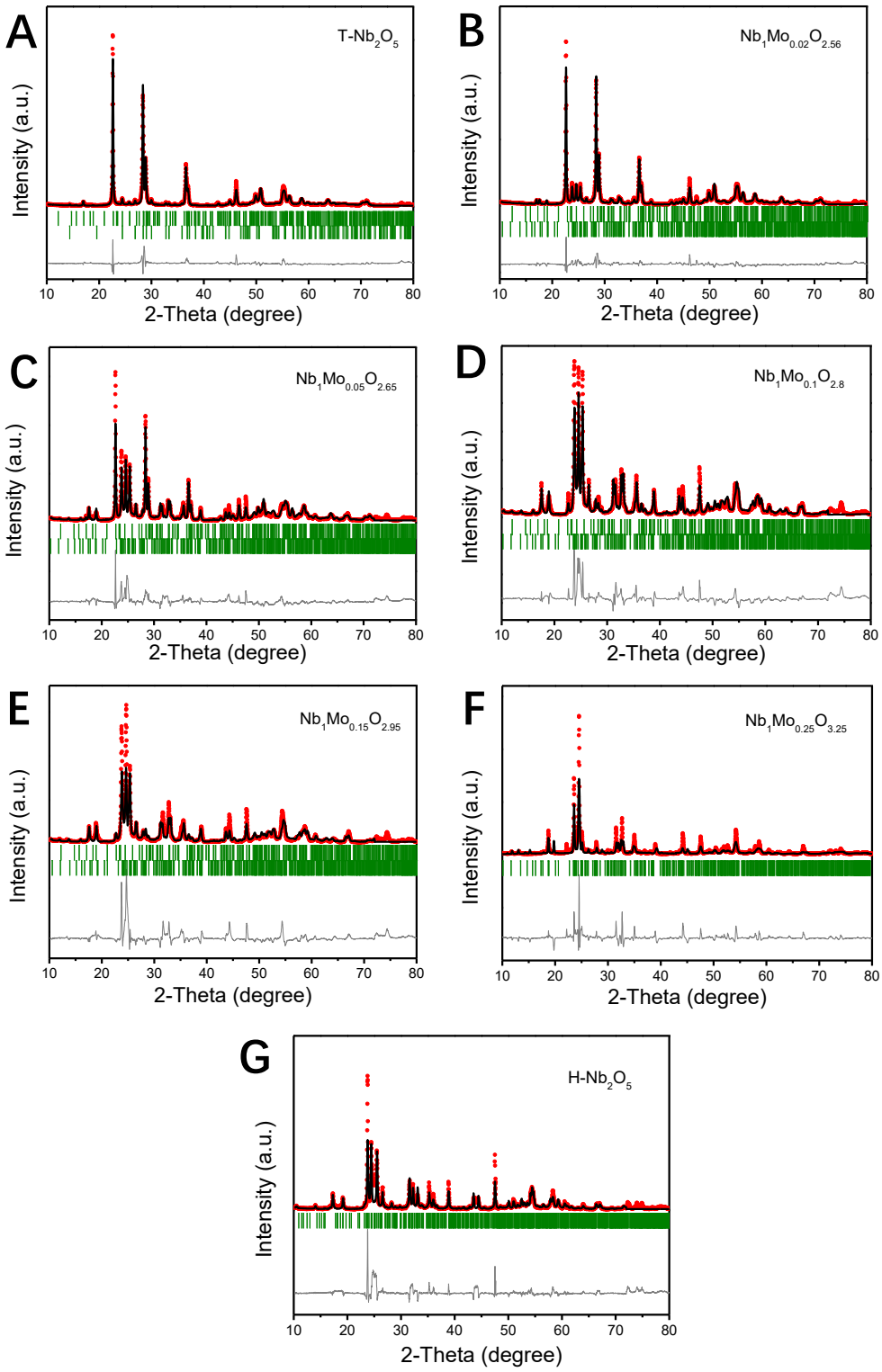

Fig. S4. XRD patterns for A, T-Nb_2O_5, B, $Nb_1Mo_{0.02}O_{2.56}$, C, $Nb_1Mo_{0.05}O_{2.65}$, D, $Nb_1Mo_{0.10}O_{2.80}$, E, $Nb_1Mo_{0.15}O_{2.95}$, F, $Nb_1Mo_{0.25}O_{3.25}$ and G, H-Nb_2O_5.

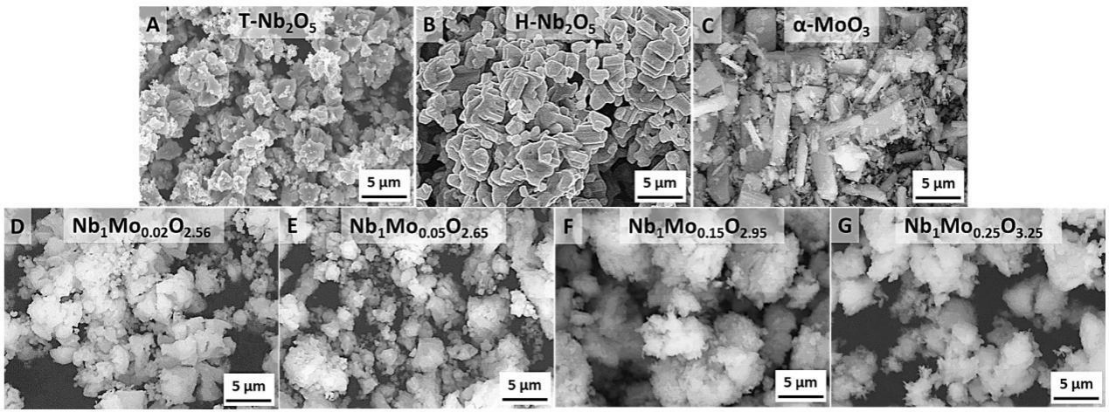

Fig. S5. SEM images of A, T-Nb_2O_5, B, H-Nb_2O_5, C, α-MoO_3, D, $Nb_1Mo_{0.02}O_{2.56}$, E, $Nb_1Mo_{0.05}O_{2.65}$, F, $Nb_1Mo_{0.15}O_{2.95}$, and G, $Nb_1Mo_{0.25}O_{3.25}$.

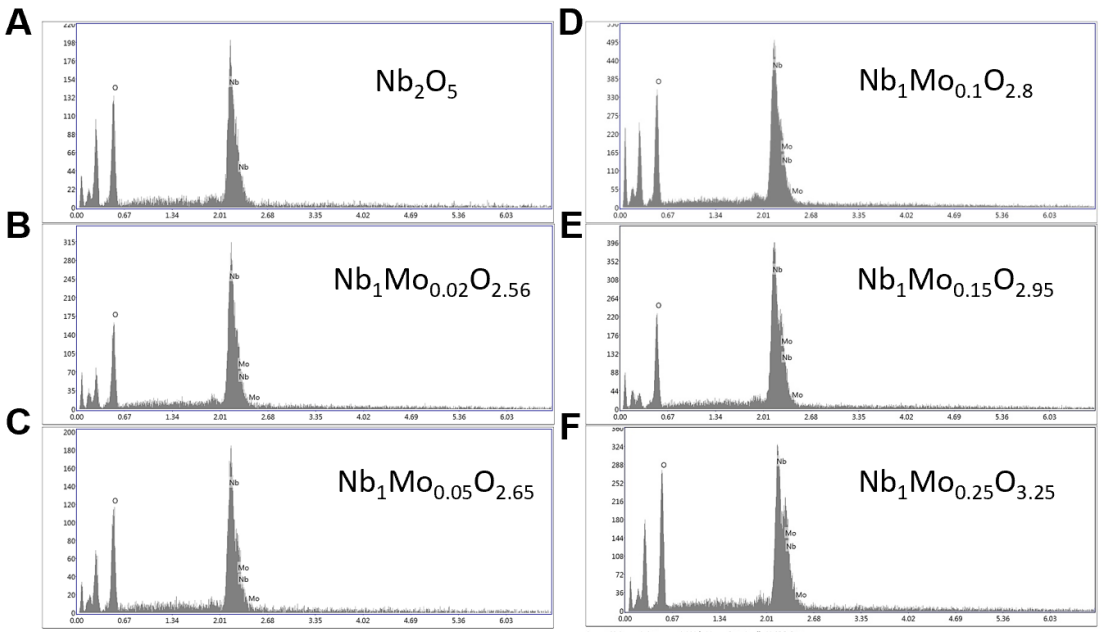

Fig. S6. EDX of as-prepared A, Nb_2O_5, B, $Nb_1Mo_{0.02}O_{2.56}$, C, $Nb_1Mo_{0.05}O_{2.65}$, D, $Nb_1Mo_{0.15}O_{2.95}$, E, $Nb_1Mo_{0.25}O_{3.25}$, and F, MoO_3.

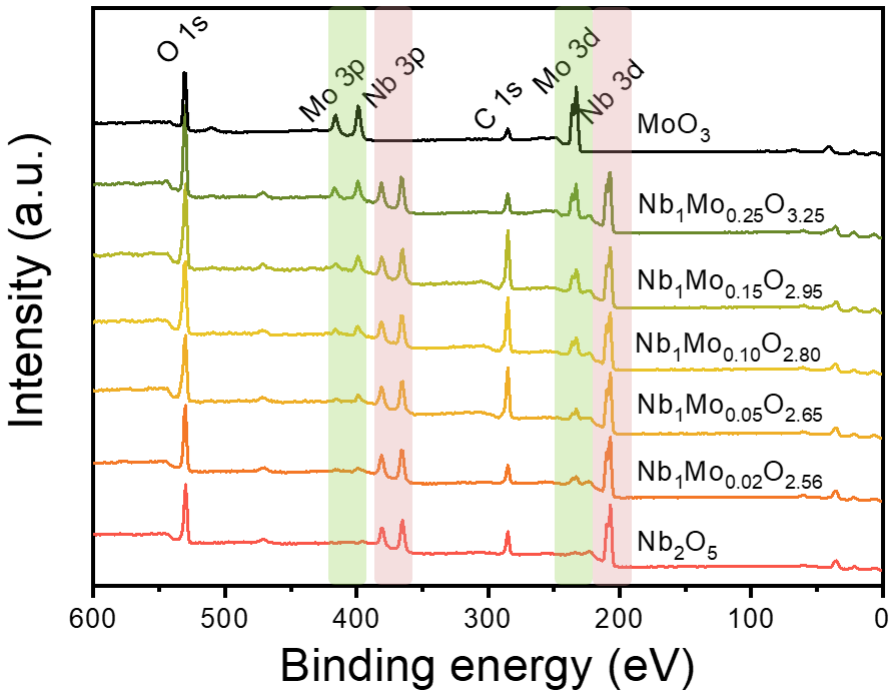

Fig. S7. XPS spectra of Nb_2O_5, $Nb_1Mo_{0.02}O_{2.56}$, $Nb_1Mo_{0.05}O_{2.65}$, $Nb_1Mo_{0.15}O_{2.95}$, $Nb_1Mo_{0.25}O_{3.25}$, and MoO_3.

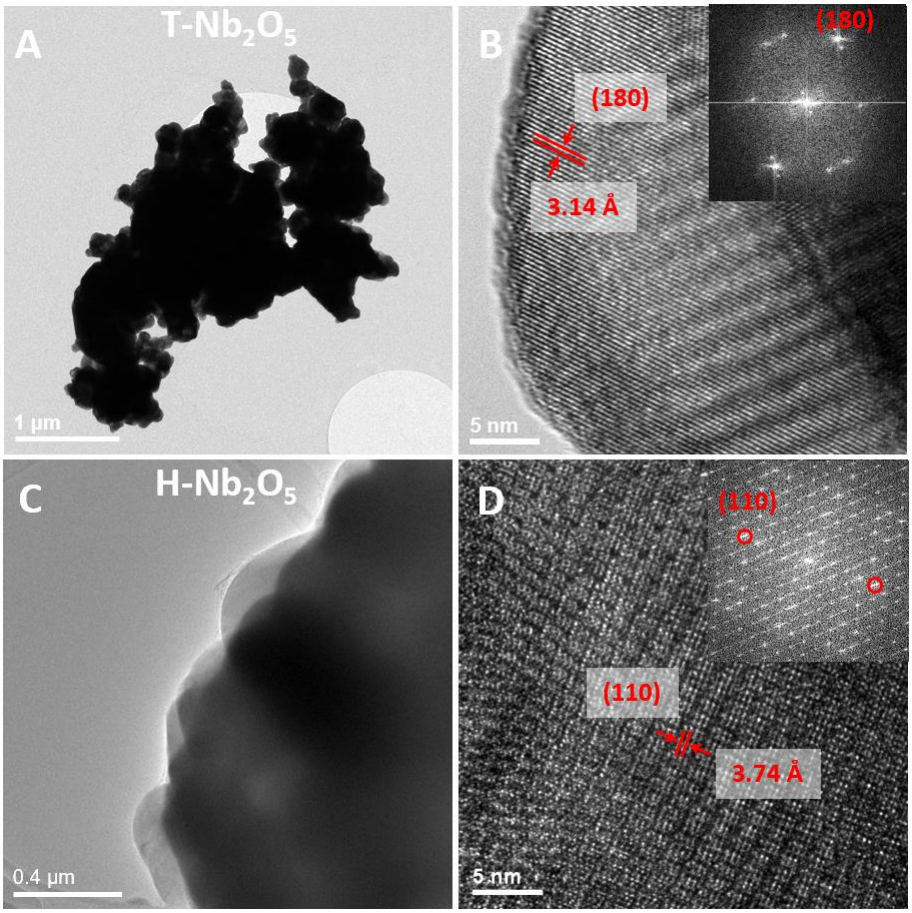

Fig. S8. TEM images of A-B, T- Nb_2O_5 and C-D, H-Nb_2O_5.

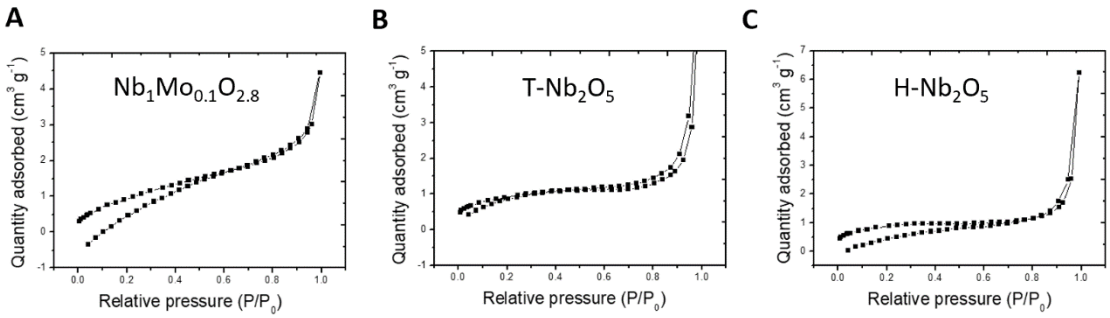

Fig. S9. BET results of A, $Nb_1Mo_{0.1}O_{2.8,}$ B, T- Nb_2O_5 and C, H-Nb_2O_5.

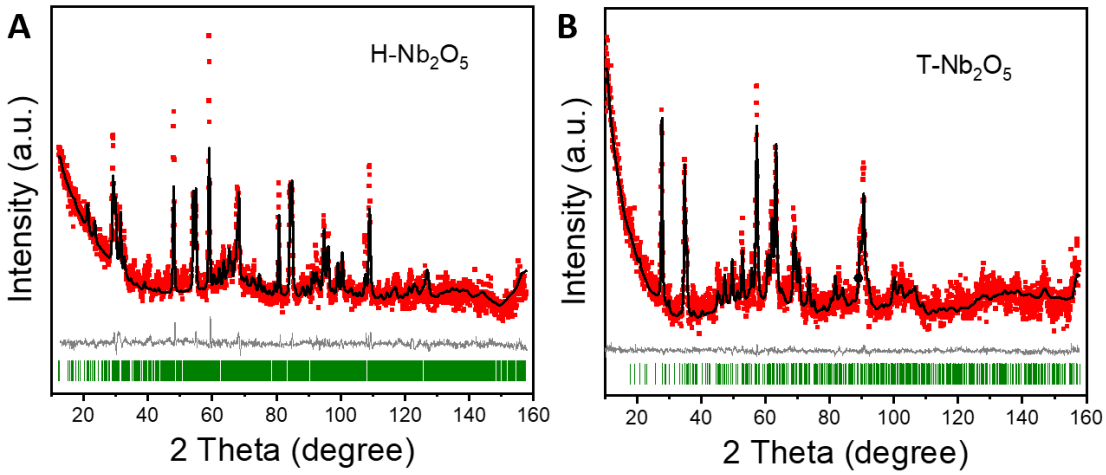

Fig. S10. The neutron powder diffraction patterns of A, H-Nb_2O_5 and B, T-Nb_2O_5.

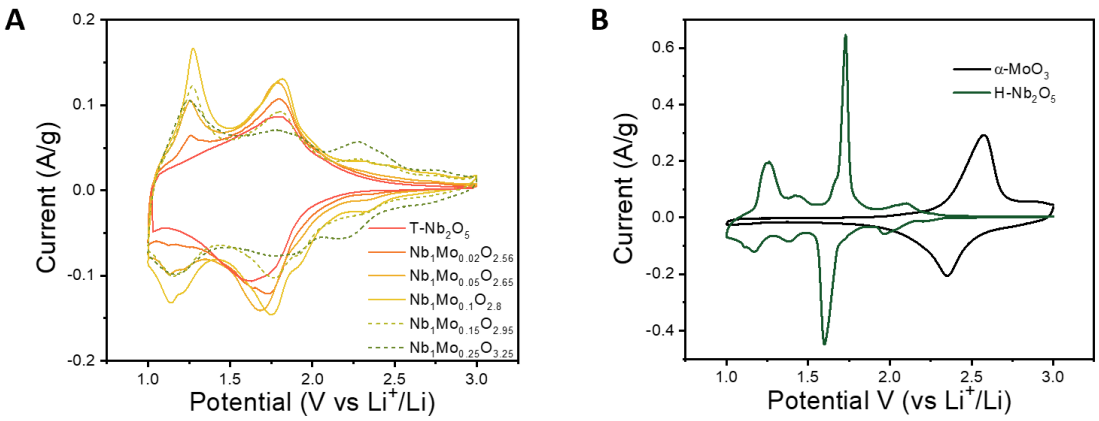

Fig. S11. A, CVs of T-Nb_2O_5, $Nb_1Mo_{0.02}O_{2.56}$, $Nb_1Mo_{0.05}O_{2.65}$, $Nb_1Mo_{0.1}O_{2.8}$, $Nb_1Mo_{0.15}O_{2.95}$, $Nb_1Mo_{0.25}O_{3.25}$. B, CVs of α-MoO_3 and H-Nb_2O_5.

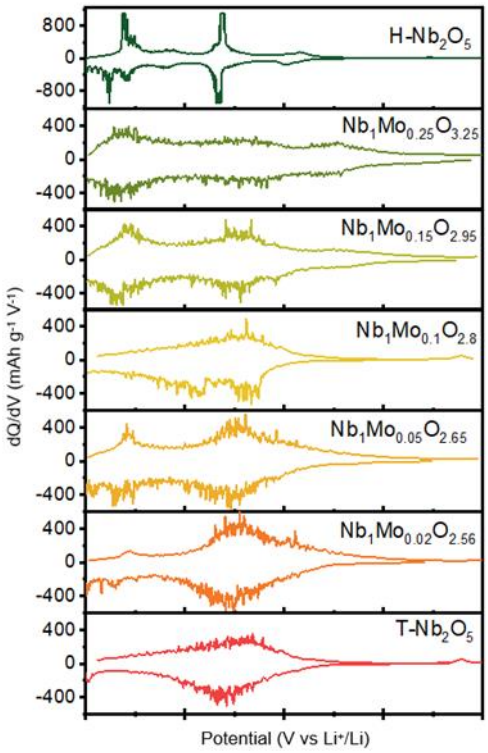

Fig. S12. The corresponding dQ/dV plots of Nb_2O_5 and Mo mixed Nb_2O_5 compounds.

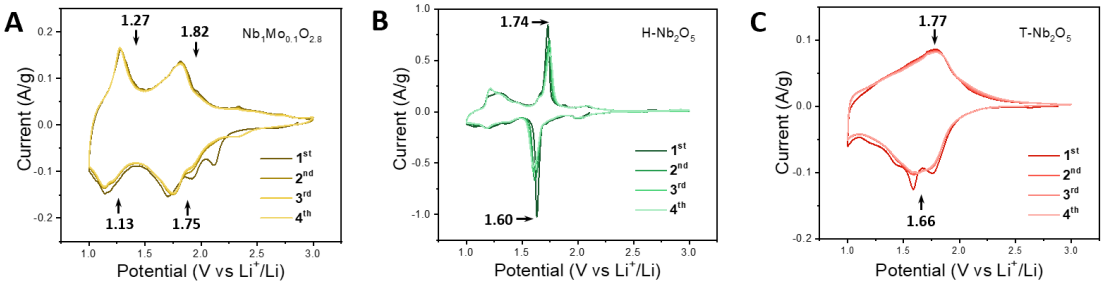

Fig. S13. First four-scan CVs of A, $Nb_1Mo_{0.1}O_{2.8}$, B, H- Nb_2O_5 and C, T-Nb_2O_5.

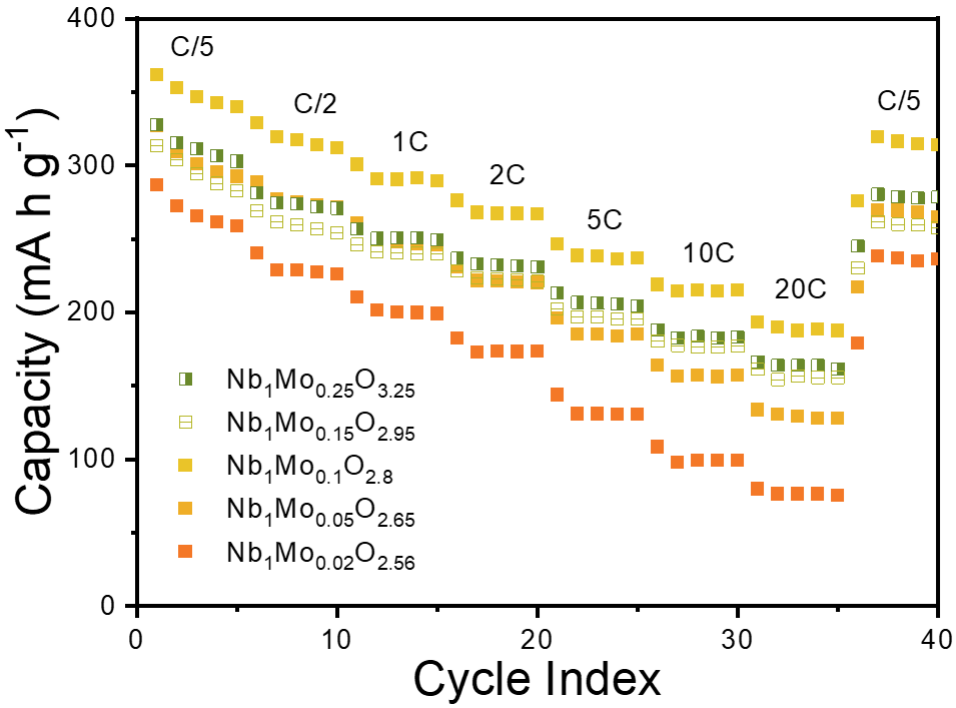

Fig. S14. Rate performance of $Nb_1Mo_{0.02}O_{2.56}$, $Nb_1Mo_{0.05}O_{2.65}$, $Nb_1Mo_{0.1}O_{2.8}$, $Nb_1Mo_{0.15}O_{2.95}$, and $Nb_1Mo_{0.25}O_{3.25}$.

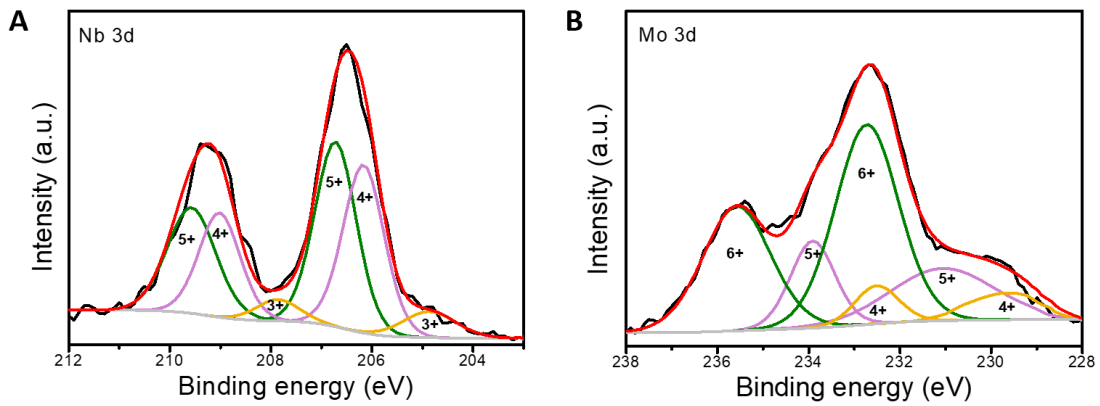

Fig. S15. Ex situ XPS spectra for A, Nb $_{3d}$ and B, Mo $_{3d}$ of $Nb_1Mo_{0.1}O_{2.8}$.

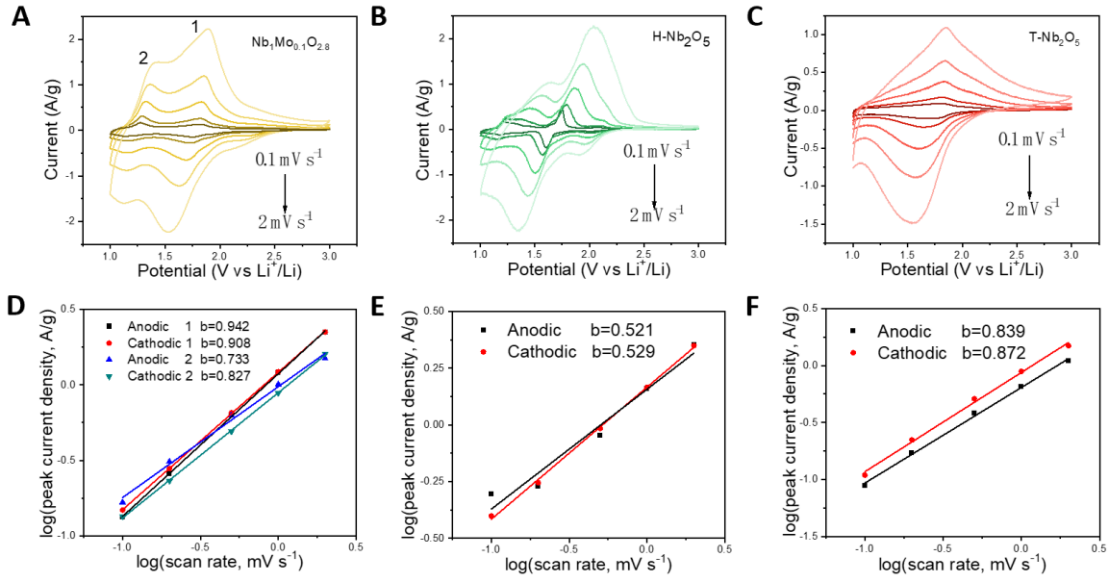

Fig. S16. CVs for A, $Nb_1Mo_{0.1}O_{2.8}$, B, H- Nb_2O_5 and C, T-Nb_2O_5. b value for D, $Nb_1Mo_{0.1}O_{2.8}$, E, H- Nb_2O_5 and F, T-Nb_2O_5.

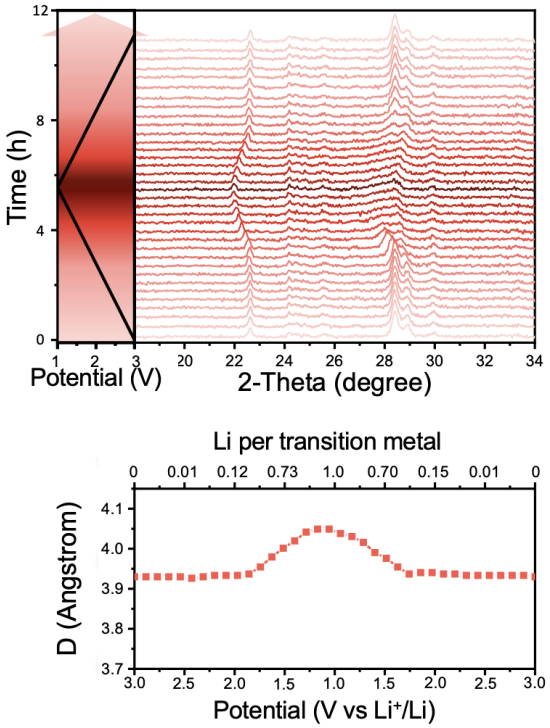

Fig. S17. *In situ* XRD test of T-Nb_2O_5 to demonstrate the structural evolution upon (de)lithiation process recorded accompanied by the cyclic voltammetry measurement at 0.1 mV s^{-1}. The lattice spacing change of the (001) plane during the in situ XRD measurement.

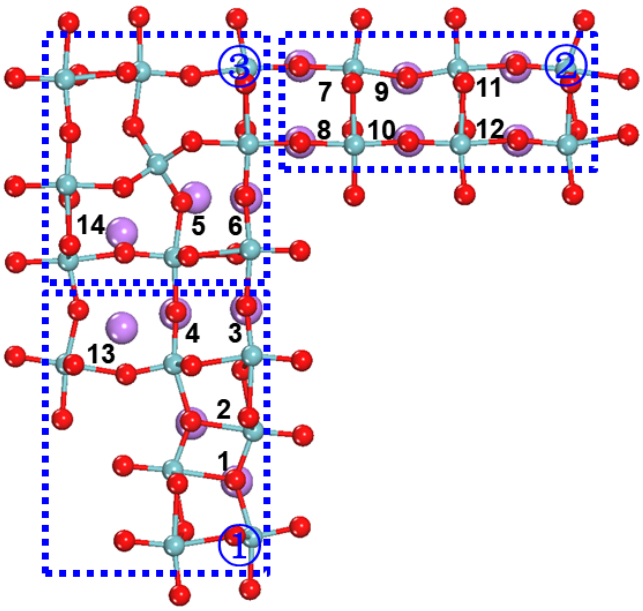

Fig. S18. Structure of lithiated H-Nb_2O_5 along edge-shared NbO_6 octahedron linked by NbO_4 tetrahedron after geometry optimization. The 14 embedded Li atoms in the mentioned above configuration are labeled, and divided into three regions, marked as "①, ②, ③". Green, red, and purple indicates Nb, O, and Li atom, respectively.

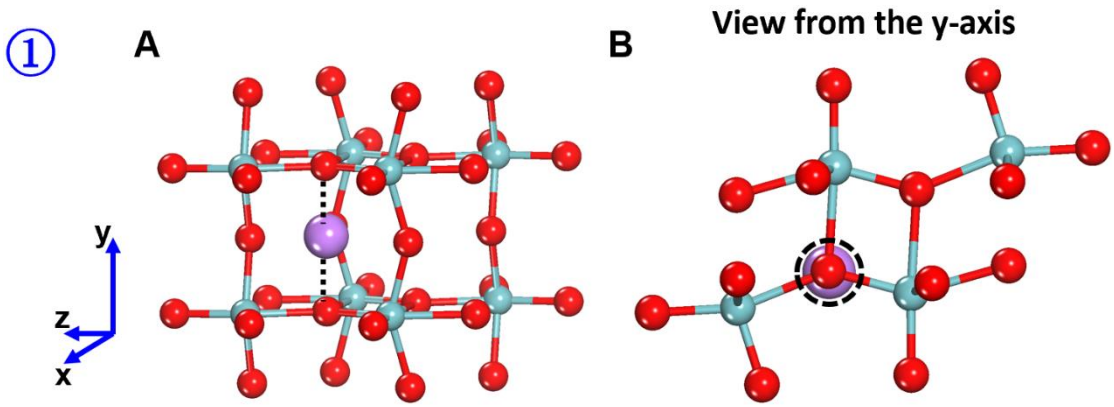

Fig. S19. A, Local bonding structure of an implanting Li atom and its neighboring atomic coordination in region "①". The bridging coordination between Li atom and O_{2e} is highlighted with purple dashed lines. B, Local bonding structure viewed from the y-axis. The Li bridged O_{2e} is marked with a purple dashed circle. Green, red, and purple represents Nb, O, and Li atom, respectively.

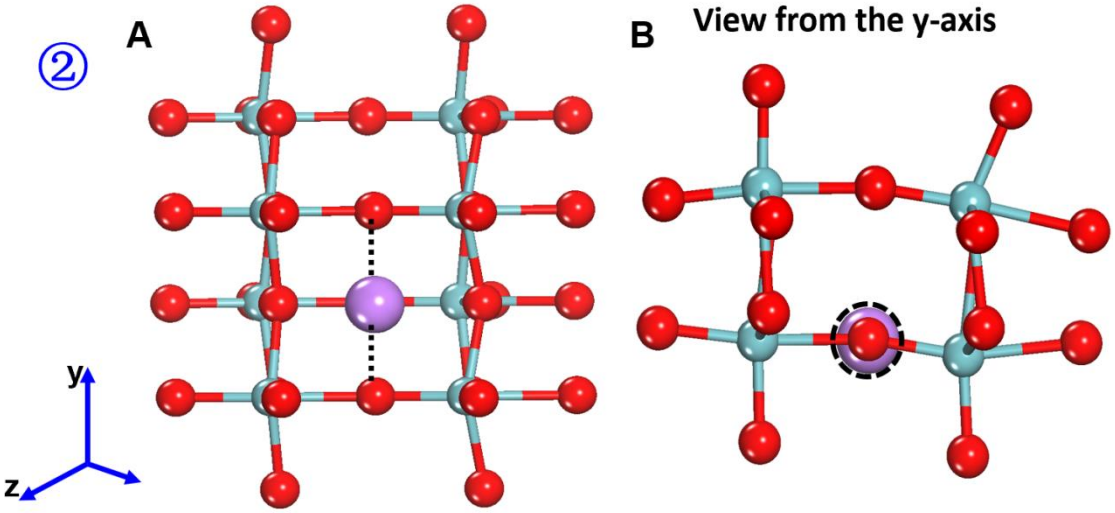

Fig. S20. A, Local bonding structure of an implanting Li atom and its neighboring atomic coordination in region "②". The bridging coordination between Li atom and O_{2e} is highlighted with purple dashed lines. B, Local bonding structure viewed from the y-axis. The Li bridged O_{2e} is marked with a purple dashed circle. Green, red, and purple represents Nb, O, and Li atom, respectively.

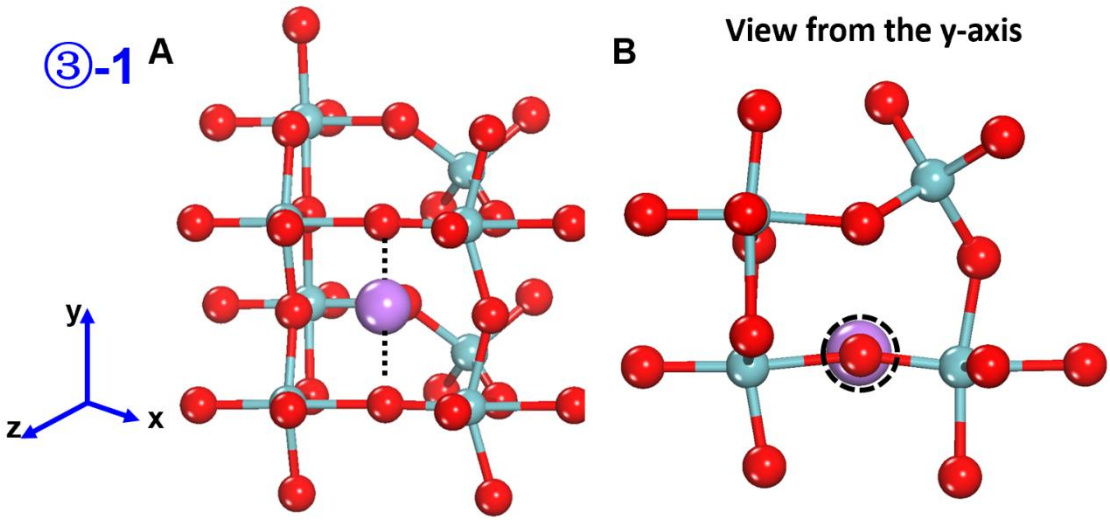

Fig. S21. A, Local bonding structure of an implanting Li atom and its neighboring atomic coordination in region "③". The bridging coordination between Li atom and O_{2e} is highlighted with purple dashed lines. B, Local bonding structure viewed from the y-axis. The Li bridged O_{2e} is marked with a purple dashed circle. Green, red, and purple represents Nb, O, and Li atom, respectively.

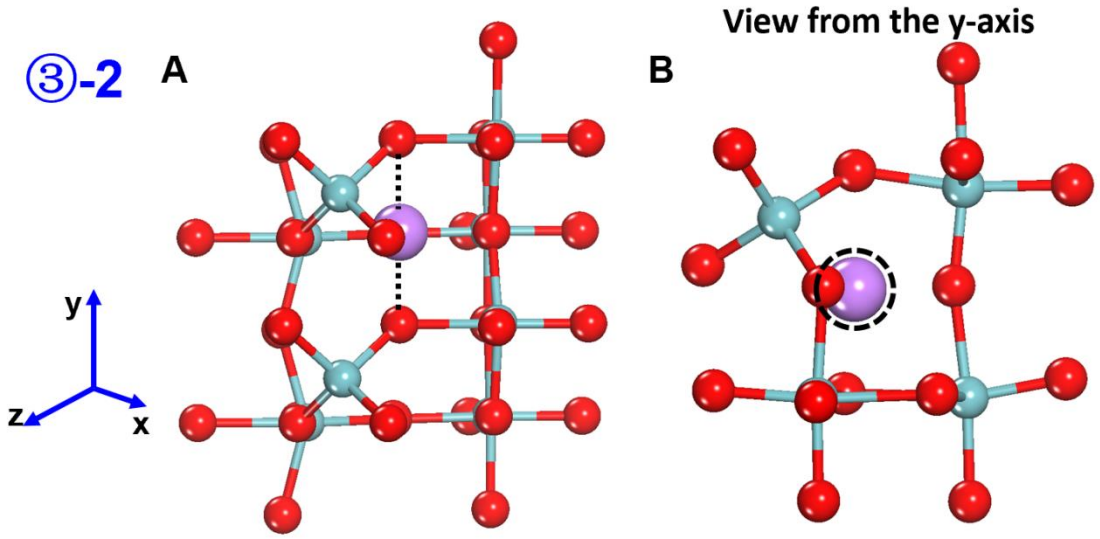

Fig. S22. A, Local bonding structure of an implanting Li atom and its neighboring atomic coordination in region "③". The bridging coordination between Li atom and O_{2e} is highlighted with purple dashed lines. B, Local bonding structure viewed from the y-axis. The Li bridged O_{2e} is marked with a purple dashed circle. Green, red, and purple represents Nb, O, and Li atom, respectively.

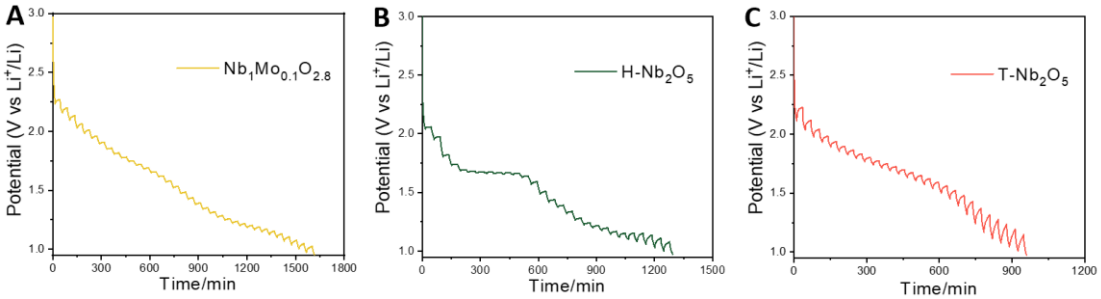

Fig. S23. GITT tests for A, $Nb_1Mo_{0.1}O_{2.8}$, B, H-Nb_2O_5, and C, T-Nb_2O_5.

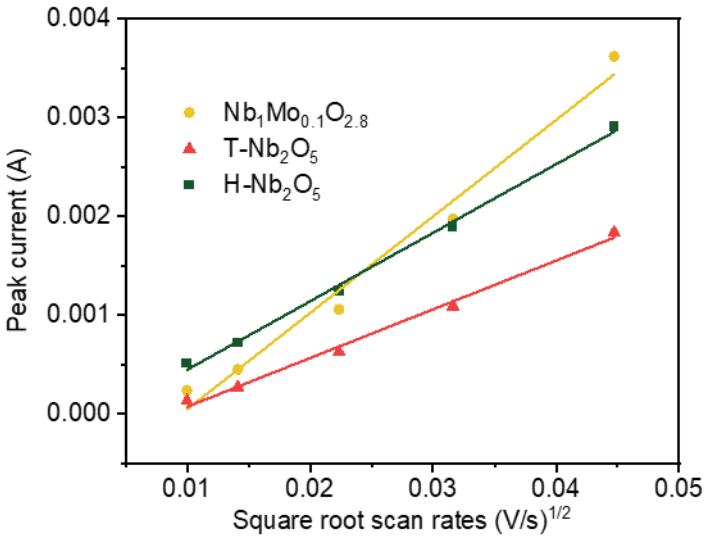

Fig. S24. The corresponding relation between the peak current and scan rate of T-and H-Nb_2O_5 and $Nb_1Mo_{0.1}O_{2.8}$ compounds. According to the Randles-Sevcik equation, the calculated diffusion coefficients were 1.53×10^{-10} ($Nb_1Mo_{0.1}O_{2.8}$), 1.88×10^{-10} (T-Nb_2O_5) and 1.33×10^{-10} (H-Nb_2O_5) $cm^2\ s^{-1}$, showing a similar trend as the values obtained from GITT analysis.

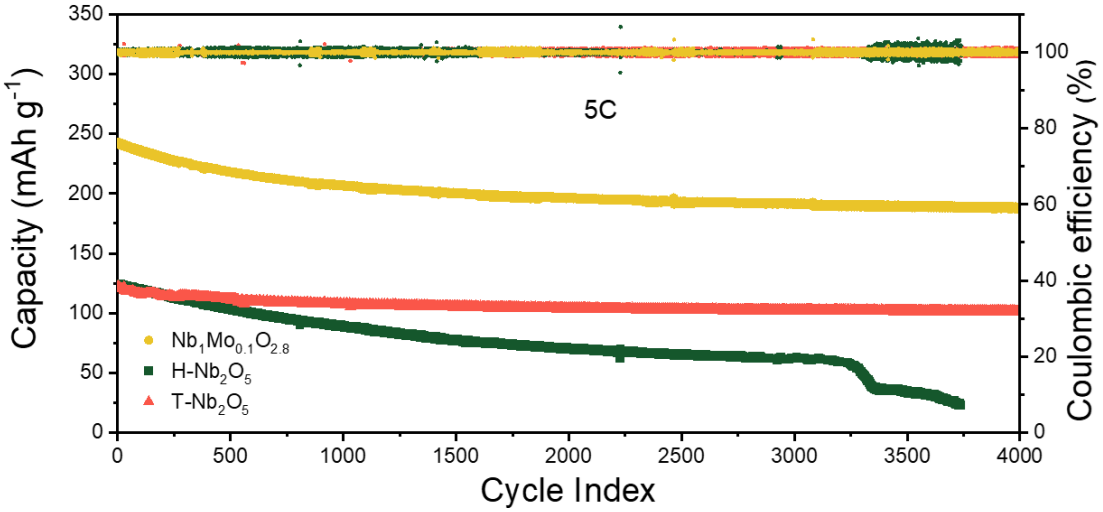

Fig. S25. Cycling stability of $Nb_1Mo_{0.1}O_{2.8}$, H- and T-Nb_2O_5.

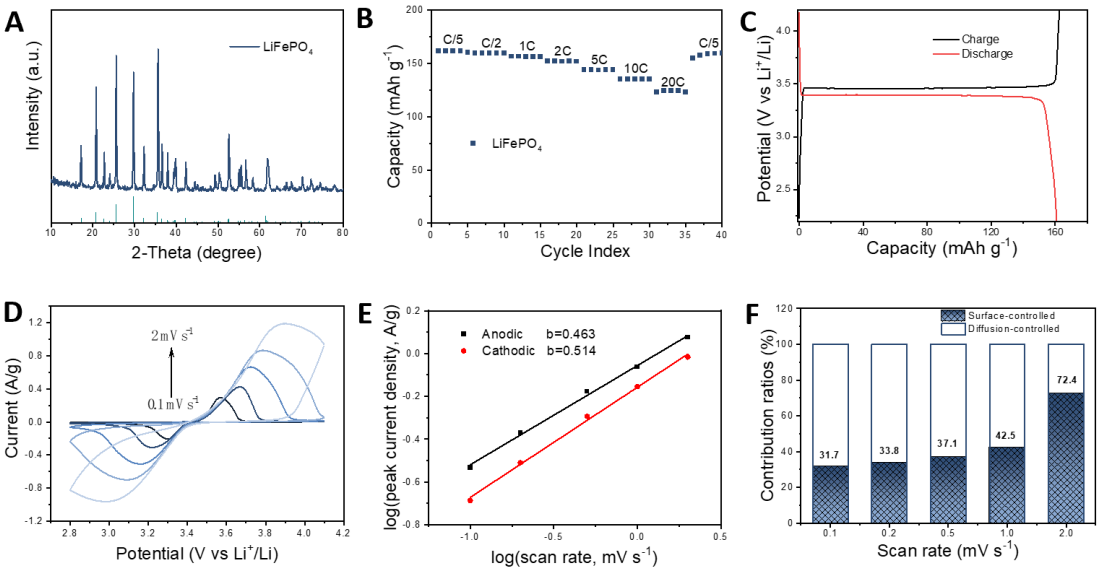

Fig. S26. A, XRD of $LiFePO_4$. B, Rate performance, C, charge/discharge curves, D, CV curves, E, b value, and F, the capacitance contribution of $LiFePO_4$ //Li half-cell.

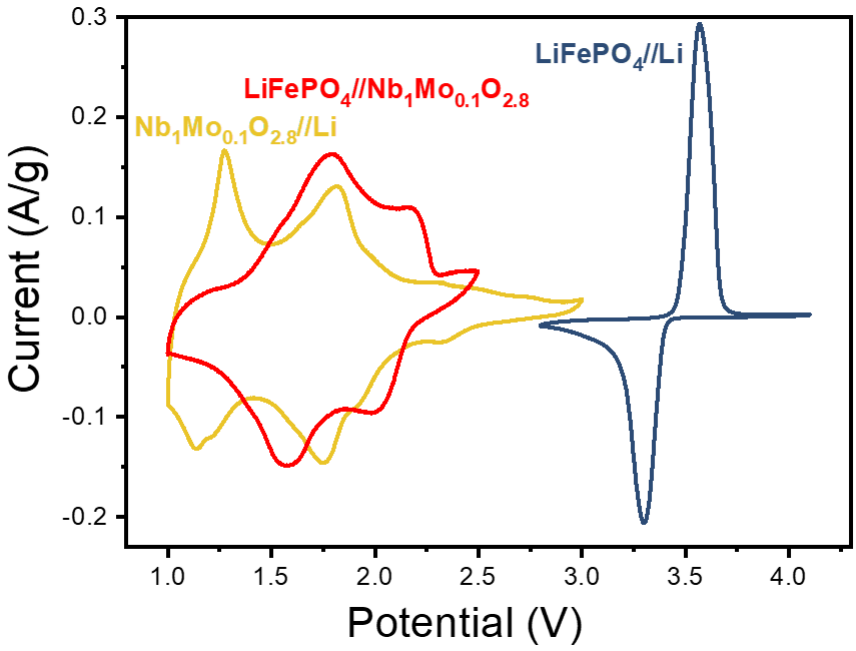

Fig. S27. CVs of $LiFePO_4$ //Li, $Nb_1Mo_{0.1}O_{2.8}$ //Li half cell and $LiFePO_4$ //$Nb_1Mo_{0.1}O_{2.8}$ full cell.

Table S1. Atomic ratios obtained from EDX spectra.

Materials	Element	Weight %	Atomic %	Net Int.	Error %
Nb_2O_5	O K	38.67	78.55	18.80	12.77
	Nb L	61.33	21.45	38.20	6.54
$Nb_1Mo_{0.02}O_{2.56}$	O K	33.77	74.77	16.70	12.73
	Nb L	64.58	24.62	43.90	5.61
	Mo L	1.64	0.61	1.00	61.24
$Nb_1Mo_{0.05}O_{2.65}$	O K	36.94	77.32	19.50	13.03
	Nb L	58.48	21.08	40.50	6.76
	Mo L	4.58	1.60	2.90	35.96
$Nb_1Mo_{0.1}O_{2.8}$	O K	27.55	68.89	8.70	10.72
	Nb L	66.16	28.49	19.10	4.71
	Mo L	6.29	2.62	1.70	17.31
$Nb_1Mo_{0.15}O_{2.95}$	O K	31.58	72.91	15.20	12.20
	Nb L	59.62	23.70	40.90	5.06
	Mo L	8.80	3.39	5.40	14.07
$Nb_1Mo_{0.25}O_{3.25}$	O K	37.75	78.01	19.70	11.63
	Nb L	48.07	17.10	32.70	5.63
	Mo L	14.18	4.89	8.80	10.49

Table S2. Refinement results of Nb_2O_5 with various Mo amount, including the structure data, phase fractions, errors and quality of fit factor.

	Structure data	T Phase Fraction（%）	B Phase Fraction（%）	H Phase Fraction（%）	Rwp
T-Nb_2O_5	T-Nb_2O_5, B-Nb_2O_5	96.16（1.08）	3.84（0.14）		16.0
$Nb_1Mo_{0.02}O_{2.56}$	T-Nb_2O_5, H-Nb_2O_5	84.09（0.92）		15.91（0.24）	15.9
$Nb_1Mo_{0.05}O_{2.65}$	T-Nb_2O_5, H-Nb_2O_5	54.18（1.15）		45.82（0.73）	23.9
$Nb_1Mo_{0.10}O_{2.80}$	T-Nb_2O_5, H-Nb_2O_5	4.43（0.33）		95.57（1.09）	26.0
$Nb_1Mo_{0.15}O_{2.95}$	T-Nb_2O_5, H-Nb_2O_5	7.43（0.07）		92.57（1.35）	33.4
$Nb_1Mo_{0.25}O_{3.25}$	T-Nb_2O_5, H-Nb_2O_5			100（0.06）	45.2
H-Nb_2O_5	H-Nb_2O_5			100（2.55）	32.9

Table S3. BET surface area of $Nb_1Mo_{0.1}O_{2.8}$, H- and T-Nb_2O_5.

Materials	Synthesis temperature (°C)	BET surface area (m^2 g^{-1})
$Nb_1Mo_{0.1}O_{2.8}$	700	3.8776
T-Nb_2O_5	700	3.2083
H-Nb_2O_5	1000	3.0724

Table S4. The performance comparison of half cell.

Materials	Potential window (V vs Li^+/Li)	Capability (mA h g^{-1})	Cycling life	References
Micro-sized T-Nb_2O_5	1.2-3.0	175 (0.1C)	~100% retention after 100 cycles (1C)	[1]
Micro-sized H-Nb_2O_5	1.2-3.0	~225 (0.1C)	<80% retention after 100 cycles (0.1C)	
Micro-sized H-Nb_2O_5	1.0-3.0	~250 (0.25C)	~83% retention after 500 cycles (10C)	[2]
Nano-sized $Ti_2Nb_{10}O_{29-x}$@C	1.0-2.5	~300 (1C)	98.7% retention after 500 cycles (10C)	[3]
Micro-sized $TiNb_2O_7$	1.0-3.0	~350 (0.2C)	>90% retention after 1,000 cycles (1C)	[4]
Micro-sized $Nb_{14}W_3O_{44}$	1.0-3.0	221.3 (0.5C)	96.5% retention after 4000 cycles (10C)	[5]
Micro-sized $Nb_{16}W_5O_{55}$	1.0-3.0	~250 (0.2C)	95% retention after 250 cycles (10C)	[6]
Nano-sized $Cr_{0.5}Nb_{24.5}O_{62}$	0.5-3.0	344 (0.1C)	92.8% retention after 1,000 cycles (10C)	[7]
Nano-sized $ZrNb_{24}O_{62}$	0.8-3.0	320 (0.1C)	90.2% retention after 1,500 cycles (10C)	[8]
Submicron-sized $V_3Nb_{17}O_{50}$	0.8-3.0	254 (0.1C)	91.8% retention over 2000 cycles (10C)	[9]
Micro-sized $Nb_1Mo_{0.1}O_{2.8}$	**1.0-3.0**	**362 (0.2C)**	**90.5% retention after 500 cycles (5C)** **80% retention after 4000 cycles (5C)**	**This work**

Table S5. Adsorption energies of Li atom labeled in Fig. S4 on the pure and Mo-doped H-Nb_2O_5 phase. The 2nd, 3rd, 4th represents the adsorption energy of pure, Mo-doped H-Nb_2O_5 phase and adsorption energy change between pure and Mo-doped H-Nb_2O_5 phase.

Label number	$E_{ads\text{-}pure}$ (eV)	$E_{ads\text{-}Mo\text{-}doped}$ (eV)	ΔE ($E_{ads\text{-}pure}$-$E_{ads\text{-}Mo\text{-}doped}$) (eV)
1	-2.64	-3.11	0.47
2	-2.64	-3.01	0.37
3	-2.90	-3.24	0.34
4	-3.35	-3.54	0.19
5	-3.29	-3.10	-0.19
6	-3.29	-3.58	0.29
7	-3.66	-3.75	0.09
8	-3.58	-3.66	0.08
9	-3.60	-3.71	0.11
10	-3.64	-3.75	0.11
11	-3.28	-3.50	0.22
12	-2.96	-3.17	0.21
13	-3.62	-3.71	0.09
14	-3.43	-3.57	0.14

Table S6. The performance comparison of full cell.

Materials	Voltage (V)	Capability (mA h g^{-1})	Cycling life	Reference
$LiFePO_4/Nb_{14}W_3O_{44}$	1.0-2.5	226.9(0.5C)	~91.9% retention after 1000 cycles (10C)	[5]
$LiFePO_4/Ti_2Nb_{10}O_{29}$	1.0-2.5	~240 (1C)	~41.7% retention after 1000 cycles (C)	[10]
$LiNi_{0.5}Mn_{1.5}O_4/Al_{0.5}Nb_{24.5}O_{62}$	1.5-3.5	~175 (5C)	89.2% retention after 800 cycles (5C)	[11]
$LiMn_2O_4/Cu_2Nb_{34}O_{87}$	1.0-3.2	229 (0.1C)	93.7% retention after 500 cycles (5C)	[12]
$LiMn_2O_4/V_3Nb_{17}O_{50}$	1.0-3.2	195(0.1C)	85.7% retention after 500 cycles (5C)	[9]
$LiFePO_4/Nb_1Mo_{0.1}O_{2.8}$	**1.0-2.5**	**278 (0.2C)**	**~88.6% retention after 1000 cycles (5C)** **~80% retention after 4000 cycles (5C)**	**This work**

References:

[1] K. J. Griffith, A. C. Forse, J. M. Griffin, C. P. Grey, *J. Am. Chem. Soc.*, **2016**, 138, 8888-8899.

[2] Z. Song, H. Li, W. Liu, H. Zhang, J. Yan, Y. Tang, J. Huang, H. Zhang, X. Li, *Adv. Mater.*, **2020**, 32, e2001001.

[3] S. Deng, H. Zhu, G. Wang, M. Luo, S. Shen, C. Ai, L. Yang, S. Lin, Q. Zhang, L. Gu, B. Liu, Y. Zhang, Q. Liu, G. Pan, Q. Xiong, X. Wang, X. Xia, J. Tu, *Nat. Commun.*, **2020**, 11, 132.

[4] K. J. Griffith, I. D. Seymour, M. A. Hope, M. M. Butala, L. K. Lamontagne, M. B. Preefer, C. P. Kocer, G. Henkelman, A. J. Morris, M. J. Cliffe, S. E. Dutton, C. P. Grey, *J. Am. Chem. Soc.*, **2019**, 141, 16706-16725.

[5] Y. Yang, H. Zhu, J. Xiao, H. Geng, Y. Zhang, J. Zhao, G. Li, X.L. Wang, C. C. Li, Q. Liu, *Adv. Mater.*, **2020**, 32, e1905295.

[6] K. J. Griffith, K. M. Wiaderek, G. Cibin, L. E. Marbella, C. P. Grey, *Nature*, **2018**, 559, 556-563.

[7] C. Yang, S. Yu, C. Lin, F. Lv, S. Wu, Y. Yang, W. Wang, Z. Z. Zhu, J. Li, N. Wang, S. Guo, *ACS Nano*, **2017**, 11, 4217-4224.

[8] C. Yang, Y. Zhang, F. Lv, C. Lin, Y. Liu, K. Wang, J. Feng, X. Wang, Y. Chen, J. Li, S. Guo, *J. Mater. Chem. A*, **2017**, 5, 22297-22304.

[9] Q. Fu, X. Zhu, R. Li, G. Liang, L. Luo, Y. Chen, Y. Ding, C. Lin, K. Wang, X. S. Zhao, *Energy Storage Mater.*, **2020**, 30, 401-411.

[10] Q. Cheng, J. Liang, Y. Zhu, L. Si, C. Guo, Y. Qian, *J. Mater. Chem. A*, **2014**, 2, 17258-17262.

[11] Q. Fu, R. Li, X. Zhu, G. Liang, L. Luo, Y. Chen, C. Lin, X. S. Zhao, *J. Mater. Chem. A*, **2019**, 7, 19862-19871.

[12] X. Zhu, G. Liang, Q. Fu, R. Li, Y. Chen, Y. Bi, D. Pan, R. Das, C. Lin, Z. Guo, *Chem. Commun.*, **2020**, 56, 7321-7324.